Ecography

ECOG-03513
Henriques-Silva, R., Kubisch, A. and Peres-Neto, P. R. 2018. Latitudinal-diversity gradients can be shaped by biotic processes: new insights from an eco-evolutionary model. – Ecography doi: 10.1111/ecog.03513

Supplementary material

Appendix 1 Population dynamics during the stationary phase

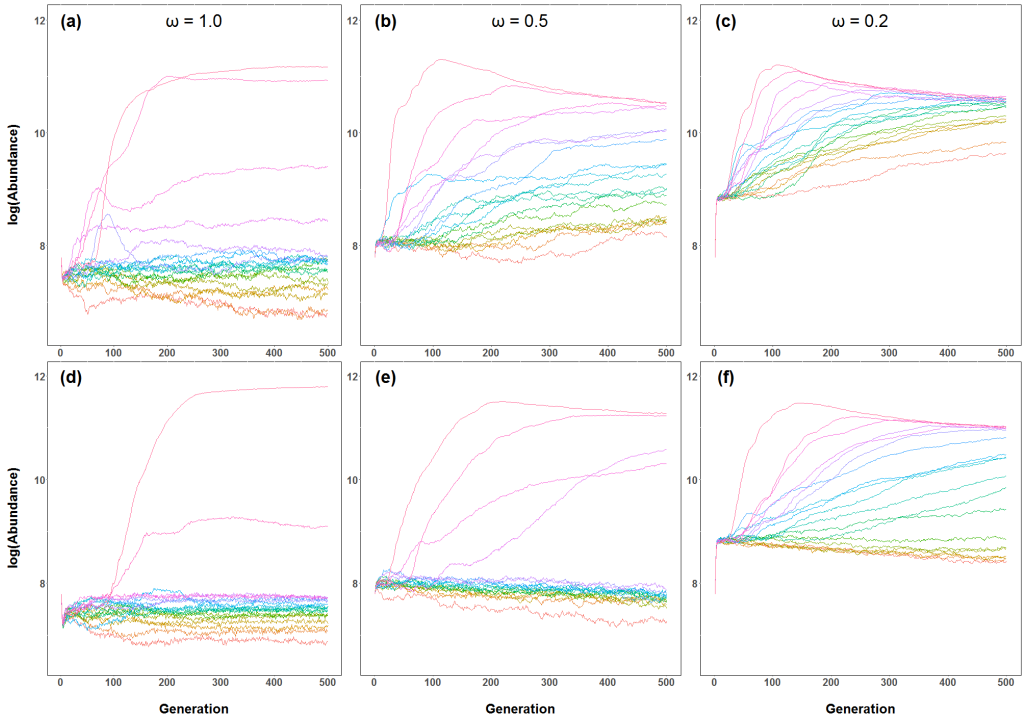

Fig A1. Species log-transformed abundance over time during the stationary phase of the simulation. The top panels represent scenarios without demographic Allee-effects (a) ω =1.0; (b) ω =0.5; (c) ω =0.2. The bottom panels represent scenarios with demographic Allee-effects (d) ω =1.0; (e) ω =0.5; (f) ω =0.2. Species where ranked by their abundances in all replicates and each colored line represents the average values across 20 replicates for each species. All species survived during this phase across all scenarios.

Appendix 2. Description of Sensitivity Analysis

A sensitivity analysis was performed to evaluate the consistency of our results regarding all relevant model parameters for all competition scenarios from our individual-based model (IBM). We followed the framework established in previous studies that used this IBM (Kubisch et al. 2011, Henriques-Silva et al. 2015). Due to computational constraints, we restricted this analysis only to species without demographic Allee effects. We also limited the number of replicates to 10 (instead of 20) for each combination of parameter change *vs* competition strength. We doubled and halved the original values of carrying capacity (K), mutation rate (m) and niche breadth (η) and evaluated the effect on each parameter of the sigmoidal curve (τ_0, β, and c) used to fit the latitudinal-diversity gradients (LDG). We also analyzed population growth rate (μ). However, we could not halve this parameter (from 2 to 1) because this would translate into null population growth in the density-dependent growth equation from Hassel (1976) used in our IBM. Instead, we added and subtracted 0.8 from the original value. The values tested are presented in table below.

Parameter	**Original Value**	+	-
K (carrying capacity)	160	320	80
*μ (population growth)	2	2.8	1.2
m (mutation rate)	0.001	0.002	0.0005
η (niche breadth)	0.5	1	0.25

*Population growth was not halved because setting it at 1 would prevent any population growth in the Hassel (1976) equation model. Instead we subtracted 0.8 from the original value. Likewise, instead of doubling, we added 0.8 to the original value.

Sigmoidal curve parameters were estimated using the R package *nls2* and we computed their average values from the 10 replicates performed on each simulation parameter modification. We then computed the difference between these average values and the ones obtained in the original simulation. Finally, we calculated sensitivity (s) as the relative change of these values divided by the relative change of the according

parameter (Kubisch et al. 2011). For instance, the sensitivity of τ_0 ($s_{\tau 0}$) to an increase in K is computed as follows:

$$s_{\tau 0} = \frac{\frac{\tau 0_{K*2} - \tau 0_{original}}{\tau 0_{original}}}{\frac{K_{*2} - K_{original}}{K_{original}}}$$

High sensitivity values indicate a higher magnitude in change on the sigmoidal parameters compared to the change in the parameter value. A positive sensitivity means that the effect on the sigmoidal parameter follows the direction of the model parameter change (e.g., an increase in a simulation parameter value causes an increase in the parameter from the sigmoidal curve). A negative sensitivity value indicates that the effect on the sigmoidal parameter goes in the opposite direction of the change in the simulation parameter value (e.g., an increase in a simulation parameter value causes a decrease in the sigmoidal parameter value). Complete results from the sensitivity analysis on sigmoidal parameters τ_0, β, and c are presented in supplementary material Appendix 3, Table A1, A2 and A3.

The first important result from the sensitivity analysis was that the asymptote of the sigmoidal curve (τ_0), which represents the maximum species diversity, was not sensitive to most parameter changes (Table A1). The only exception was found in the scenario with the strongest competitive interactions ($\omega = 1.0$) where the estimated τ_0 were lower than in the original simulation, especially under lower carrying capacity (K –) and population growth rates (μ –) (Table A1). In these cases, some species went extinct during the simulation (*results not shown*) which consequently decreased the maximum diversity (i.e., the asymptote of the curve; see Fig. A2d). Indeed lower values of both

parameters makes species more susceptible to extinction, especially if they have to cope with strong biotic interactions.

The steepness of the curve at the inflection point (β; Table A2), which represents diversity-decline rates, was slightly more sensitive to parameter change than τ_0. Still, it was affected by model parameter change only under ω = 0.6, 0.8 and 1.0 (i.e., the three scenarios with the strongest competitive interactions; Table A2). The strongest sensitivity was found under changes in population growth rates (μ) in the strongest competition scenario (ω = 1.0). The diversity-decline under lower population growth rates (μ –) was much smoother than in the main simulation. As we said in the previous paragraph, some species went extinct in this particular scenario, which decreased the maximum diversity (see Fig. A2d). This resulted on a smoother diversity decline because there was a lower maximum diversity to decline from. Higher mutation rates (*m* +) and larger niche breadth (η +) consistently resulted in smoother diversity decline whereas lowering these parameters (*m* – and η –) resulted in a steeper diversity decline. Not surprisingly, when the abiotic constraints are relaxed (i.e., higher local adaptation capability), more species are able to expand their ranges across the gradient. Likewise, when the abiotic constraints are increased (i.e., lower mutation rates and narrow niche breadth), less species are able to expand. Change in these parameters did not affect diversity-decline (β) in the scenarios with weak competitive interactions (ω = 0.2 and 0.3).

Finally, the inflection point (*c*) was the most affected parameter on our sensitivity analysis, with the exception of the scenario with very strong competitive interactions ω = 1.0 (Table A3). The inflection point represents the portion of the latitudinal-diversity curve when the diversity is halved. In general, this portion was farther from the initial

southern regions (i.e., larger c) when carrying capacity (K), mutation rates (m) and niche breadth (η) increased (+) and growth rates (μ) decreased (–). When these parameters were changed in the other direction, the inflection point was closer to the southern regions (i.e., smaller c). Mirroring the results from the diversity decline rates (β), more (less) species were able to expand under higher (lower) mutation rates and wider (narrower) niche breadths due to a higher (lower) potential for local adaptation, which led to a larger (smaller) c. However, this process did not happen in the scenario with the strongest competitive interactions (Table A1). In this case, the biotic constraints were so important that it did not matter that species were better (or worse) in their local adaptation capacity. Likewise, changing the carrying capacity (K) under strong competitive interactions did not influence c (sensitivity = 0; Table A1), but it affected the estimated inflection point in other competition scenarios. Larger values of K result in larger c because it dampens the effect of interspecific competition and allows more species to expand farther across the landscape (Table A1; Figure A2). In the same way, lower carrying capacity (K) amplifies the effect of interspecific competition and results in smaller c. Finally, population growth rates (μ) affected c by the same mechanisms. Larger μ results in more individuals and hence stronger competition among species. This led to lower c values as less species are able to expand their ranges across the landscape. Likewise, lower μ values have the opposite effect on c (Table A3).

While the sensitivity analysis showed that the magnitude of the results from our main simulation can be sensitive to these IBM parameters, it did not affect our general conclusion. In all cases, more species were able to expand under weak competitive interactions and vice-versa (see Figure A2).

Appendix 3. Parameter estimation of the sigmoidal curve in each simulation parameter change from the sensitivity analysis

Table A1. Results of the sensitivity analysis on τ_0 (i.e., the asymptote of the curve). Values presented are averages from the estimated τ_0 values of the 10 replicates for each parameter change. The table also shows the difference between τ_0 values from the scenarios with parameter change and the scenario from the main simulation and the sensitivity of this difference relative to the parameter change. ε = standard error; p = p-value.

Scenario	Parameter change	τ_0	ε	p	Difference	Sensitivity
ω =1.0	Original	20	1.443	<0.0001	--	--
	K +	20	1.438	<0.0001	0	0
	K –	16	1.458	<0.0001	4	0.4
	μ +	17	1.214	<0.0001	3	-0.375
	μ –	11	1.829	<0.0001	9	1.125
	m +	19	1.492	<0.0001	1	-0.05
	m –	19	1.189	<0.0001	1	0.1
	η +	19	1.771	<0.0001	1	-0.05
	η –	19	1.063	<0.0001	1	0.1
ω =0.8	Original	20	2.57	<0.0001	--	--
	K +	20	2.305	<0.0001	0	0
	K –	20	2.951	<0.0001	0	0
	μ +	19	6.421	0.0048	1	-0.125
	μ –	20	1.751	<0.0001	0	0
	m +	20	3.523	<0.0001	0	0
	m –	20	2.186	<0.0001	0	0
	η +	20	2.576	<0.0001	0	0
	η –	20	1.924	<0.0001	0	0
ω =0.6	Original	20	2.16	<0.0001	--	--
	K +	20	3.716	<0.0001	0	0
	K –	20	2.513	<0.0001	0	0
	μ +	20	5.076	0.0003	0	0
	μ –	20	2.207	<0.0001	0	0
	m +	20	3.502	<0.0001	0	0
	m –	20	2.633	<0.0001	0	0
	η +	20	3.322	<0.0001	0	0
	η –	20	2.43	<0.0001	0	0
ω =0.5	Original	20	2.981	<0.0001	--	--
	K +	20	2.265	<0.0001	0	0
	K –	20	3.777	<0.0001	0	0
	μ +	20	3.374	<0.0001	0	0
	μ –	20	1.356	<0.0001	0	0
	m +	20	2.41	<0.0001	0	0
	m –	20	3.961	<0.0001	0	0
	η +	20	2.041	<0.0001	0	0
	η –	20	2.609	<0.0001	0	0
ω =0.3	Original	20	0.957	<0.0001	--	--
	K +	20	0.6	<0.0001	0	0
	K –	20	1.433	<0.0001	0	0
	μ +	19	1.346	<0.0001	1	-0.125
	μ –	20	0.305	<0.0001	0	0

	$m+$	20	0.603	<0.0001	0	0
	$m-$	20	1.348	<0.0001	0	0
	$\eta+$	20	0.549	<0.0001	0	0
	$\eta-$	20	2.036	<0.0001	0	0
ω =0.2	Original	20	0.286	<0.0001	--	--
	$K+$	20	0.171	<0.0001	0	0
	$K-$	20	0.526	<0.0001	0	0
	$\mu+$	19	0.587	<0.0001	1	-0.125
	$\mu-$	20	0.157	<0.0001	0	0
	$m+$	20	0.181	<0.0001	0	0
	$m-$	20	0.548	<0.0001	0	0
	$\eta+$	20	0.173	<0.0001	0	0
	$\eta-$	20	0.832	<0.0001	0	0

Table A2. Results of the sensitivity analysis on β (i.e., the steepness of the curve at the inflection point). Values presented are averages from the estimated β values of the 10 replicates for each parameter change. The table also shows the difference between β values from the scenarios with parameter change and the scenario from the main simulation and the sensitivity of this difference relative to the parameter change. ε = standard error; p = p-value.

Scenario	Parameter change	β	ε	p	Difference	Sensitivity
ω =1.0	Original	-0.278	0.052	<0.0001	--	--
	K +	-0.304	0.062	<0.0001	0.025	0.091
	K –	-0.253	0.054	<0.0001	-0.025	0.182
	μ +	-0.532	0.15	0.0009	0.253	2.273
	μ –	-0.051	0.009	<0.0001	-0.228	2.045
	m +	-0.278	0.057	<0.0001	0	0
	m –	-0.329	0.063	<0.0001	0.051	-0.364
	η +	-0.228	0.044	<0.0001	-0.051	-0.182
	η –	-0.43	0.095	<0.0001	0.152	-1.091
ω =0.8	Original	-0.076	0.015	<0.0001	--	--
	K +	-0.076	0.015	<0.0001	0	0
	K –	-0.076	0.015	<0.0001	0	0
	μ +	-0.051	0.01	<0.0001	-0.025	-0.833
	μ –	-0.051	0.008	<0.0001	-0.025	0.833
	m +	-0.051	0.011	<0.0001	-0.025	-0.333
	m –	-0.101	0.019	<0.0001	0.025	-0.667
	η +	-0.051	0.009	<0.0001	-0.025	-0.333
	η –	-0.127	0.024	<0.0001	0.051	-1.333
ω =0.6	Original	-0.051	0.01	<0.0001	--	--
	K +	-0.025	0.005	<0.0001	-0.025	-0.5
	K –	-0.051	0.01	<0.0001	0	0
	μ +	-0.025	0.004	<0.0001	-0.025	-1.25
	μ –	-0.025	0.004	<0.0001	-0.025	1.25
	m +	-0.025	0.005	<0.0001	-0.025	-0.5
	m –	-0.051	0.01	<0.0001	0	0
	η +	-0.025	0.005	<0.0001	-0.025	-0.5
	η –	-0.076	0.017	<0.0001	0.025	-1
ω =0.5	Original	-0.025	0.005	<0.0001	--	--
	K +	-0.025	0.004	<0.0001	0	0
	K –	-0.025	0.005	<0.0001	0	0
	μ +	-0.025	0.004	<0.0001	0	0
	μ –	-0.025	0.003	<0.0001	0	0
	m +	-0.025	0.004	<0.0001	0	0
	m –	-0.025	0.005	<0.0001	0	0
	η +	-0.025	0.004	<0.0001	0	0
	η –	-0.051	0.011	<0.0001	0.025	-2
ω =0.3	Original	-0.025	0.003	<0.0001	--	--
	K +	-0.025	0.002	<0.0001	0	0
	K –	-0.025	0.004	<0.0001	0	0
	μ +	-0.025	0.004	<0.0001	0	0
	μ –	-0.025	0.001	<0.0001	0	0
	m +	-0.025	0.002	<0.0001	0	0
	m –	-0.025	0.003	<0.0001	0	0
	η +	-0.025	0.002	<0.0001	0	0
	η –	-0.025	0.004	<0.0001	0	0
ω =0.2	Original	-0.025	0.002	<0.0001	--	--
	K +	-0.025	0.001	<0.0001	0	0
	K –	-0.025	0.002	<0.0001	0	0
	μ +	-0.025	0.003	<0.0001	0	0

	μ −	-0.051	0.003	<0.0001	0.025	-2.5
	m +	-0.025	0.002	<0.0001	0	0
	m −	-0.025	0.002	<0.0001	0	0
	η +	-0.025	0.002	<0.0001	0	0
	η −	-0.025	0.003	<0.0001	0	0

Table A3. Results of the sensitivity analysis on *c* (i.e., the inflection point). Values presented are averages from the estimated *c* values of the 10 replicates for each parameter change. The table also shows the difference between *c* values from the scenarios with parameter change and the scenario from the main simulation and the sensitivity of this difference relative to the parameter change. ε = standard error; p = p-value.

Scenario	Parameter change	c	ε	p	Difference	Sensitivity
ω =1.0	Original	12.41	0.908	<0.0001	--	--
	K +	12.41	0.876	<0.0001	0	0
	K –	12.41	1.194	<0.0001	0	0
	μ +	10	0.639	<0.0001	2.405	-0.485
	μ –	31.65	8.191	0.0003	-19.241	-3.878
	m +	12.41	0.988	<0.0001	0	0
	m –	12.41	0.741	<0.0001	0	0
	η +	12.41	1.283	<0.0001	0	0
	η –	12.41	0.611	<0.0001	0	0
ω =0.8	Original	29.24	4.699	<0.0001	--	--
	K +	31.65	4.343	<0.0001	-2.405	0.082
	K –	24.43	5.077	<0.0001	4.81	0.329
	μ +	12.41	13.89	0.3764	16.835	-1.439
	μ –	48.48	4.971	<0.0001	-19.241	-1.645
	m +	34.05	8.858	0.0004	-4.81	0.165
	m –	24.43	3.137	<0.0001	4.81	0.329
	η +	38.86	6.747	<0.0001	-9.62	0.329
	η –	22.03	2.334	<0.0001	7.215	0.494
ω =0.6	Original	50.89	6.256	<0.0001	--	--
	K +	60.51	17.971	0.0015	-9.62	0.189
	K –	43.67	6.854	<0.0001	7.215	0.284
	μ +	31.65	21.516	0.148	19.241	-0.945
	μ –	79.75	11.524	<0.0001	-28.861	-1.418
	m +	62.91	17.111	0.0006	-12.025	0.236
	m –	43.67	7.181	<0.0001	7.215	0.284
	η +	65.32	16.389	0.0002	-14.43	0.284
	η –	34.05	4.716	<0.0001	16.835	0.662
ω =0.5	Original	70.13	14.995	<0.0001	--	--
	K +	79.75	11.826	<0.0001	-9.62	0.137
	K –	58.1	18.081	0.0024	12.025	0.343
	μ +	48.48	15.485	0.003	21.646	-0.772
	μ –	98.99	7.564	<0.0001	-28.861	-1.029
	m +	79.75	12.584	<0.0001	-9.62	0.137
	m –	58.1	18.962	0.0036	12.025	0.343
	η +	84.56	10.844	<0.0001	-14.43	0.206
	η –	46.08	7.26	<0.0001	24.051	0.686
ω =0.3	Original	123.04	5.694	<0.0001	--	--
	K +	139.87	3.672	<0.0001	-16.835	0.137
	K –	103.8	8.116	<0.0001	19.241	0.313
	μ +	108.61	8.135	<0.0001	14.43	-0.293
	μ –	156.71	1.906	<0.0001	-33.671	-0.684
	m +	144.68	3.717	<0.0001	-21.646	0.176
	m –	103.8	7.634	<0.0001	19.241	0.313
	η +	144.68	3.381	<0.0001	-21.646	0.176
	η –	86.96	10.914	<0.0001	36.076	0.586
ω =0.2	Original	168.73	1.851	<0.0001	--	--
	K +	190.38	1.466	<0.0001	-21.646	0.128
	K –	147.09	3.251	<0.0001	21.646	0.257
	μ +	159.11	3.882	<0.0001	9.62	-0.143
	μ –	183.16	1.143	<0.0001	-14.43	-0.214
	m +	195.19	1.752	<0.0001	-26.456	0.157
	m –	144.68	3.374	<0.0001	24.051	0.285
	η +	195.19	1.673	<0.0001	-26.456	0.157

	η –	127.85	4.996	<0.0001	40.886	0.485

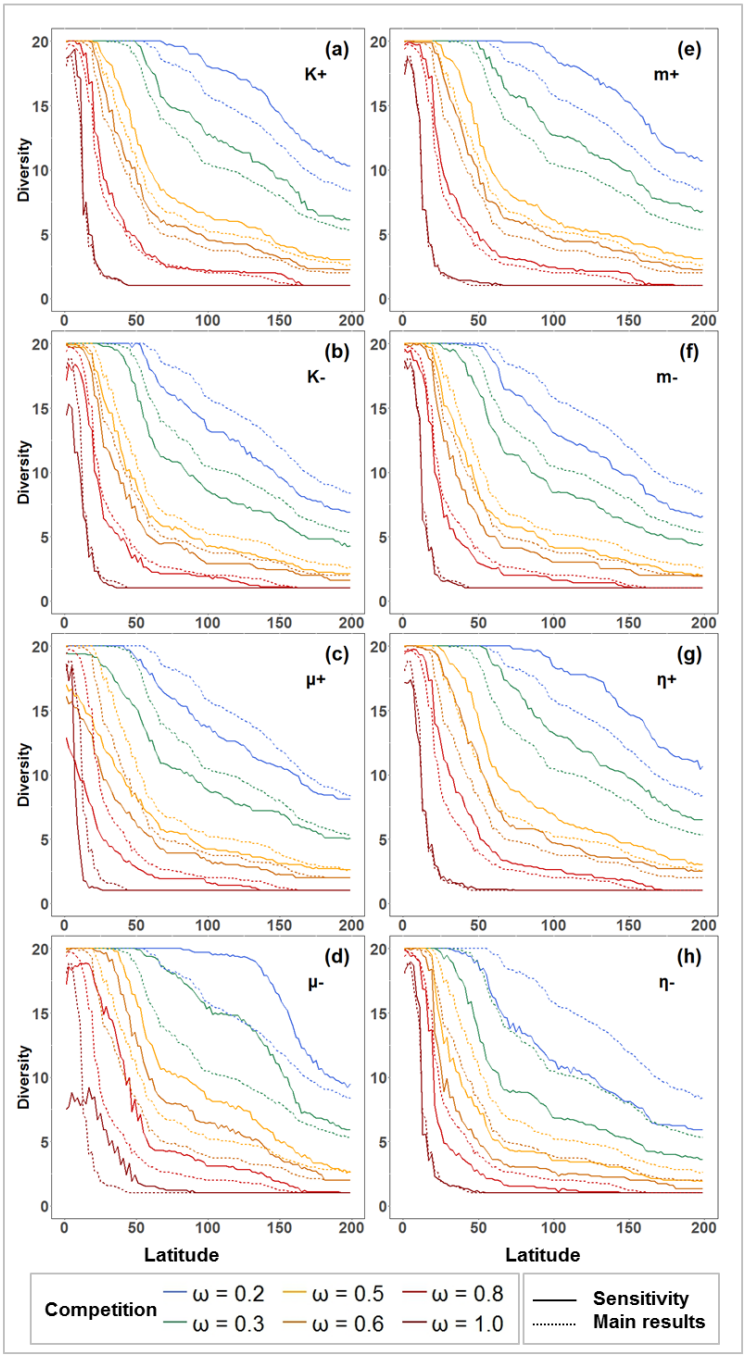

Fig A2. Results from the sensitivity analysis. Relationship between species diversity and latitude (*y*-axis) for species without demographic Allee for different parameter changes: (a) *K*+ (320), (b) *K*– (80), (c) μ+ (2.8), (d) μ– (1.2), (e) *m*+ (0.002), (f) *m*– (0.0005), (g) η+ (1) and η– (0.5). Each colored line represents the average result of the 10 replicates for each competition scenario. Solid lines represent the results from the sensitivity analysis whereas dashed lines represent the values obtained in the main simulation. Hence, all dashed lines are the same in every panel. Parameter values from the sigmoidal function in each scenario are presented in Table A1, A2 and A3.

Appendix 4 Count histograms from the geographic range size (GRS)

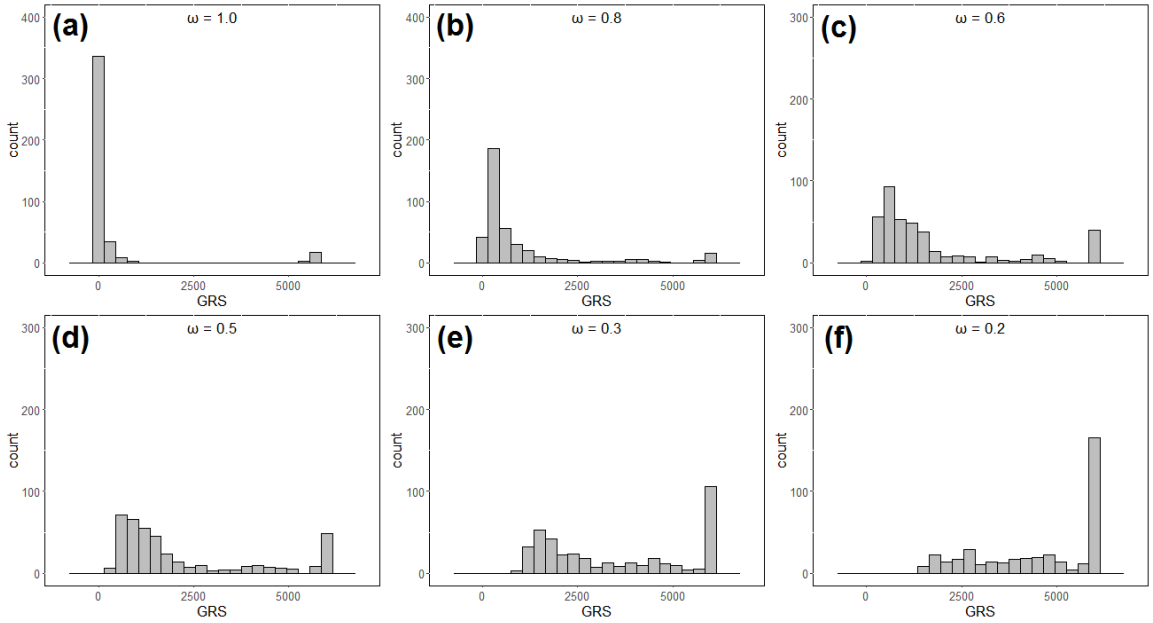

Fig. A3. Count histograms from the geographic range size (GRS) distributions of species without demographic Allee-effects. Data was pooled from all species across all replicates for each scenario of interspecific competition. (a) ω = 1.0, skewness = 4.03; (b) ω = 0.8, skewness = 2.31; (c) ω = 0.6, skewness = 1.35; (d) ω = 0.5, skewness = 0.97; (e) ω = 0.3, skewness = 0.16; (f) ω = 0.2, skewness = -0.45.

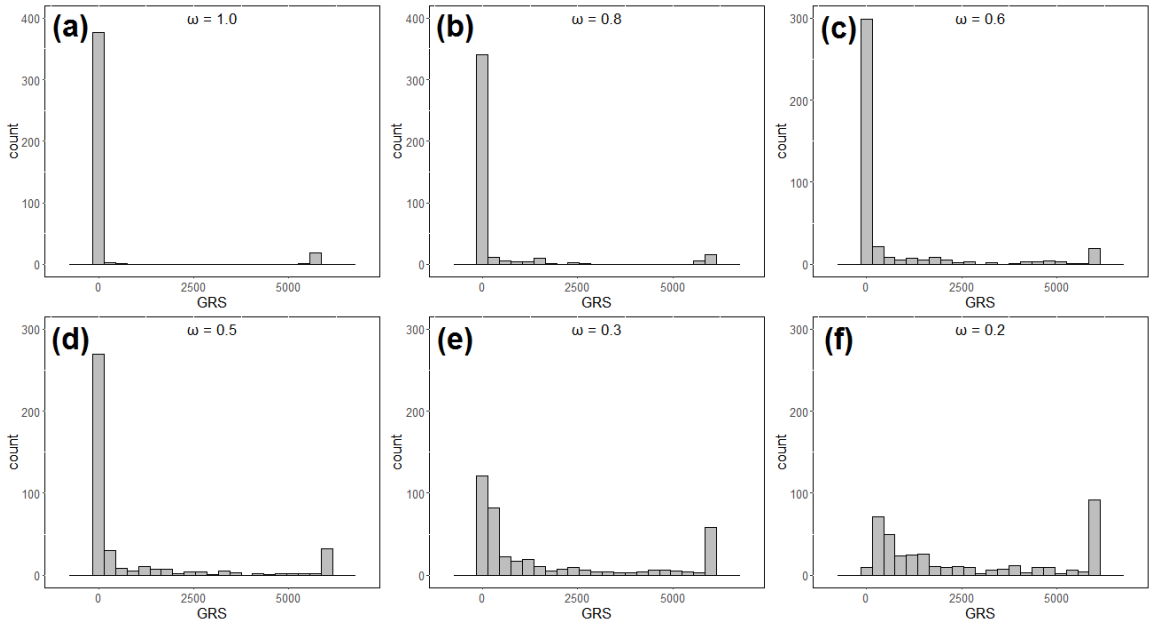

Fig. A4. Count histograms from the geographic range size (GRS) distributions of species subjected to demographic Allee-effect. Data was pooled from all species across all replicates for each scenario of interspecific competition. (a) ω = 1.0, skewness = 4.11; (b) ω = 0.8, skewness = 3.48; (c) ω = 0.6, skewness = 2.23; (d) ω = 0.5, skewness = 1.81; (e) ω = 0.3, skewness = 0.83; (f) ω = 0.2, skewness = 0.27.

Appendix 5 Range expansion and dispersal and environmental traits eco-evolutionary dynamics during the expansion phase

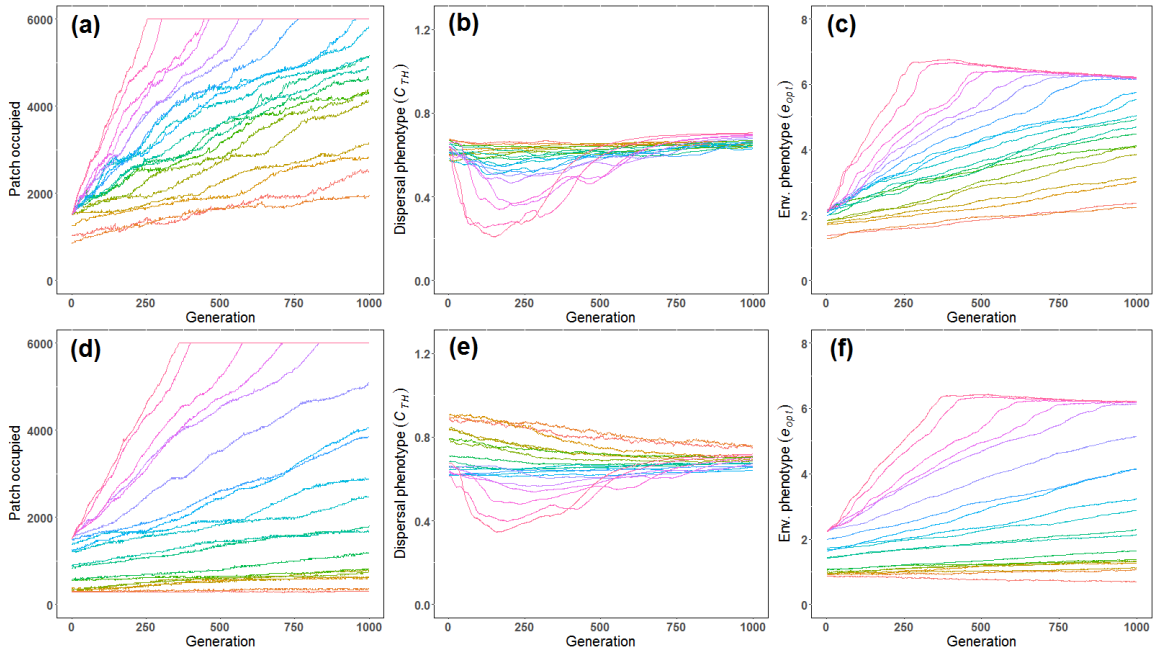

Fig. A5. Results for range expansion speed (a, d), dispersal evolution (b, e) and niche evolution (c, f) for the competition scenario ω = 0.2. Panels in the top and bottom rows refer to scenarios without and with demographic Allee effects, respectively. Species where ranked by their abundances in all replicates and each colored line represents the average values across replicates for each species. The light pink line represents the fastest species, which is the first to attain the patch # 6000 in panel (a). Range expansion panels show the farthest occupied patch in which the species was found in generation *t*. Dispersal evolution panels show the average value of the dispersal phenotype (***d***) for each species across time. Finally, niche evolution panels show the average value of the environmental optima phenotype (e_{opt}) for each species across time.

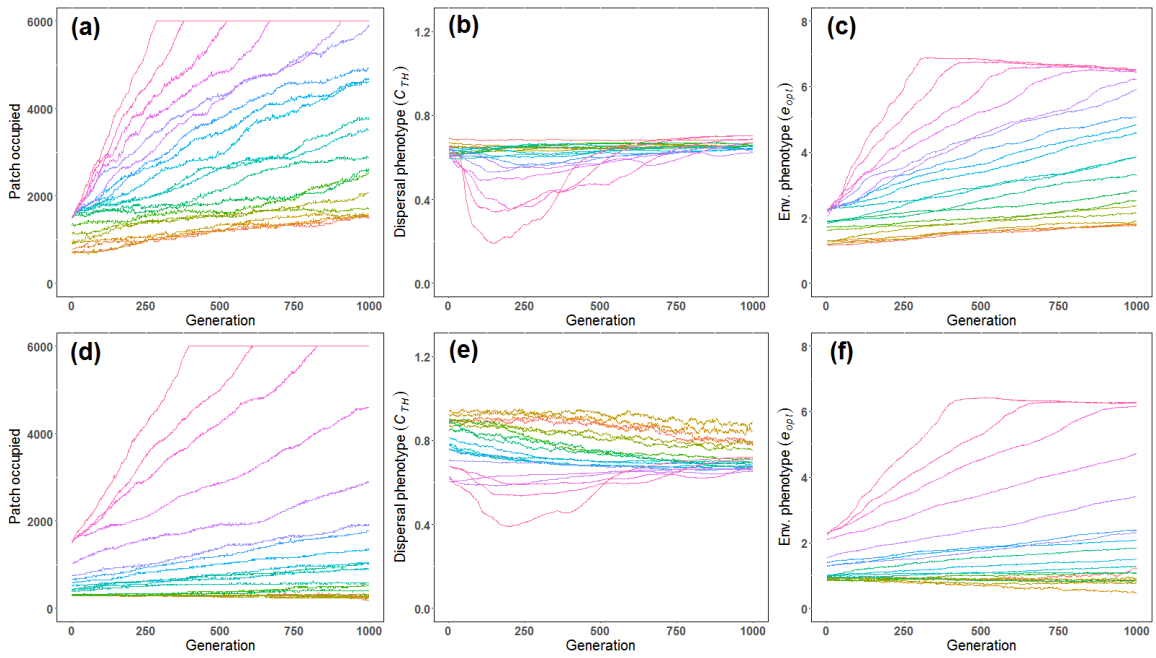

Fig. A6. Results for range expansion speed (a, d), dispersal evolution (b, e) and niche evolution (c, f) for the competition scenario ω = 0.3. Panels in the top and bottom rows refer to scenarios with out and with demographic Allee effects, respectively. Species where ranked by their abundances in all replicates and each colored line represents the average values across replicates for each species. The light pink line represents the fastest species, which is the first to attain the patch # 6000 in panel (a). Range expansion panels show the farthest occupied patch in which the species was found in generation *t*. Dispersal evolution panels show the average value of the dispersal phenotype (***d***) for each species across time. Finally, niche evolution panels show the average value of the environmental optima phenotype (e_{opt}) for each species across time.

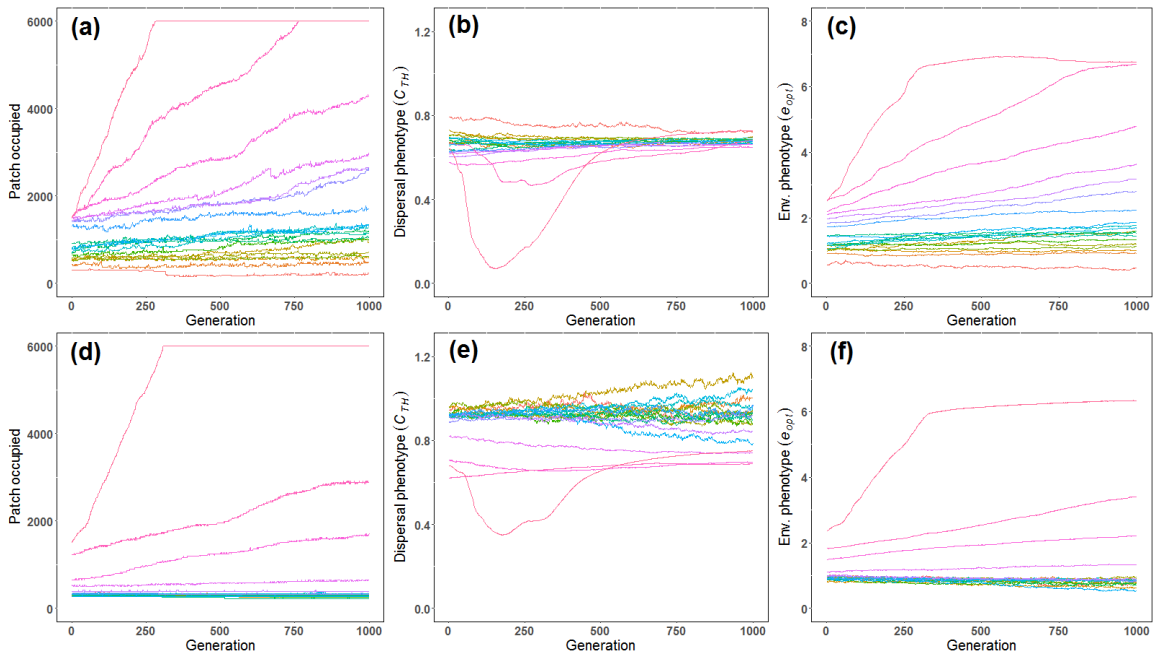

Fig. A7. Results for range expansion speed (a, d), dispersal evolution (b, e) and niche evolution (c, f) for the competition scenario ω = 0.6. Panels in the top and bottom rows refer to scenarios with out and with demographic Allee effects, respectively. Species where ranked by their abundances in all replicates and each colored line represents the average values across replicates for each species. The light pink line represents the fastest species, which is the first to attain the patch # 6000 in panel (A). Range expansion panels show the farthest occupied patch in which the species was found in generation *t*. Dispersal evolution panels show the average value of the dispersal phenotype (***d***) for each species across time. Finally, niche evolution panels show the average value of the environmental optima phenotype (e_{opt}) for each species across time.

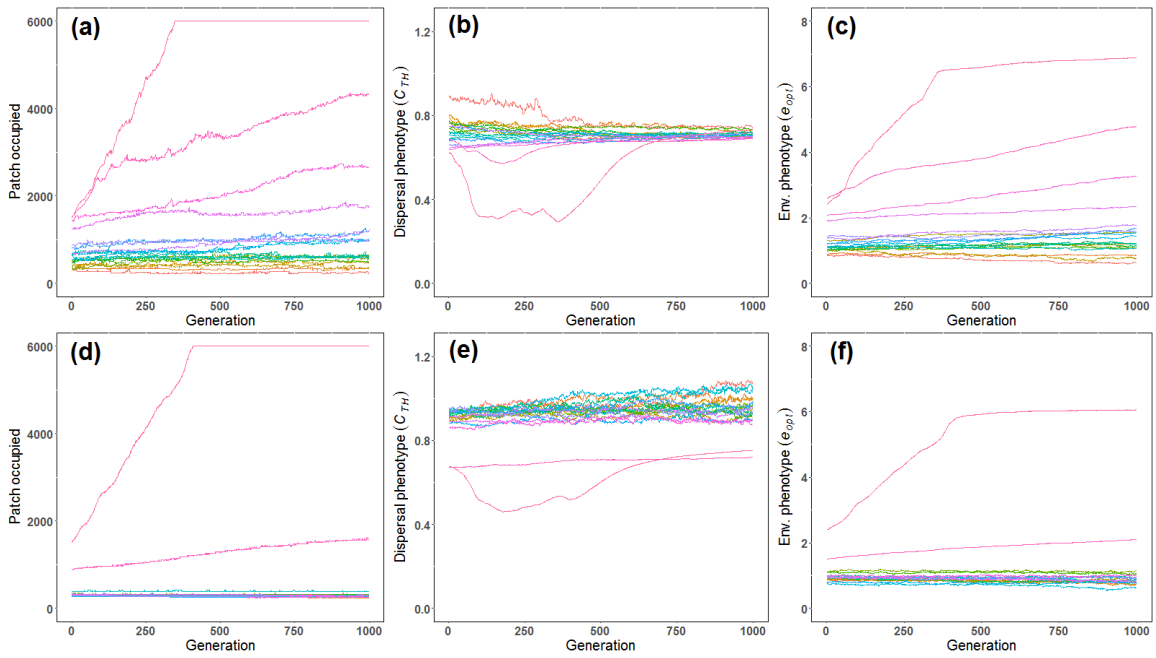

Fig. A8. Results for range expansion speed (a, d), dispersal evolution (b, e) and niche evolution (c, f) for the competition scenario ω = 0.8. Panels in the top and bottom rows refer to scenarios without and with demographic Allee effects, respectively. Species where ranked by their abundances in all replicates and each colored line represents the average values across replicates for each species. The light pink line represents the fastest species, which is the first to attain the patch # 6000 in panel (a). Range expansion panels show the farthest occupied patch in which the species was found in generation *t*. Dispersal evolution panels show the average value of the dispersal phenotype (***d***) for each species across time. Finally, niche evolution panels show the average value of the environmental optima phenotype (e_{opt}) for each species across time.

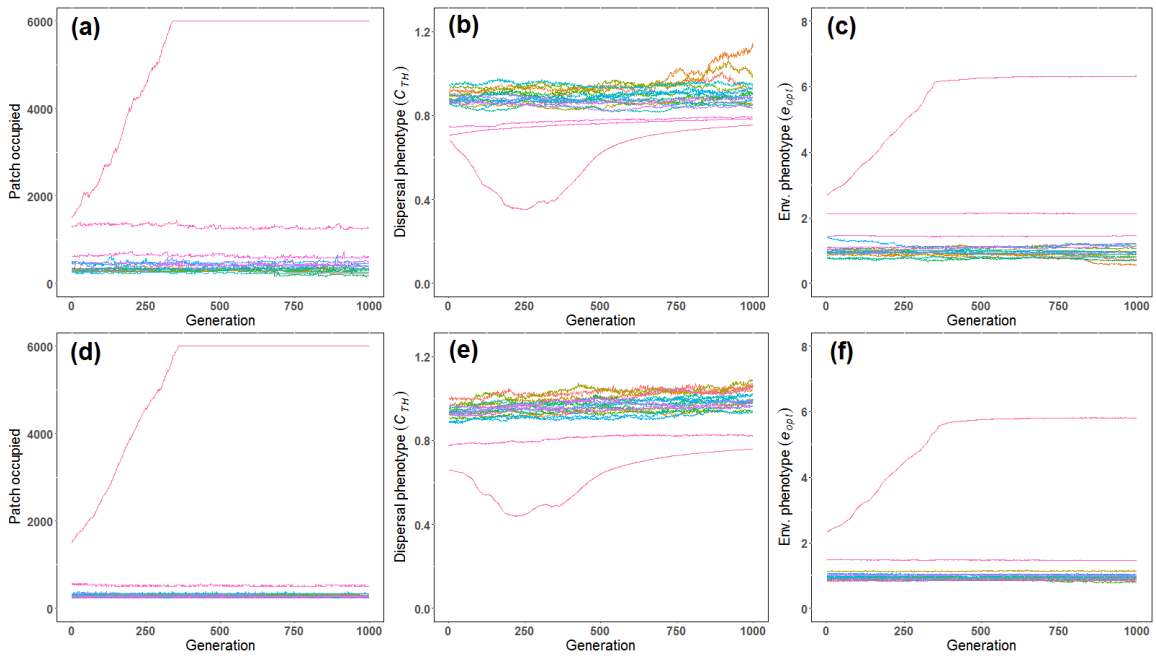

Fig. A9. Results for range expansion speed (a, d), dispersal evolution (b, e) and niche evolution (c, f) for the competition scenario ω = 1.0. Panels in the top and bottom rows refer to scenarios without and with demographic Allee effects, respectively. Species where ranked by their abundances in all replicates and each colored line represents the average values across replicates for each species. The light pink line represents the fastest species, which is the first to attain the patch # 6000 in panel (a). Range expansion panels show the farthest occupied patch in which the species was found in generation *t*. Dispersal evolution panels show the average value of the dispersal phenotype (***d***) for each species across time. Finally, niche evolution panels show the average value of the environmental optima phenotype (e_{opt}) for each species across time.

Appendix 6 – Simulation experiment with a longer (i.e., 4000 generations) expansion phase

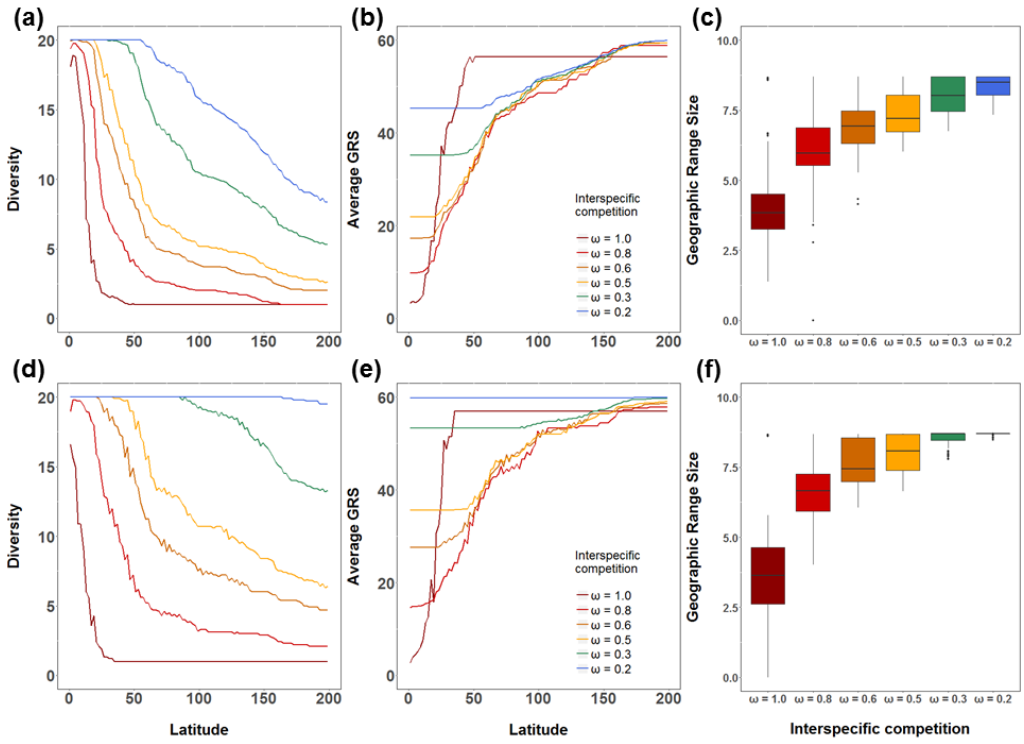

Figure A10. Main results from the simulation experiment with a longer expansion phase (4000 generations; bottom panels) contrasted with the original results (1000 generations; top panels) for the group of species not subjected to Allee effects. Diversity gradients (a, d), average geographic range size (GRS) gradients (e, f) and species average GRS (c, f). Each color represents a different competition scenario (see legend in panels e and f). The results were fairly similar in respect to the differences across competition scenarios. The only distinction appeared in scenarios with very low competition intensity (ω = 0.2 and ω = 0.3) where the diversity and GRS gradients almost disappeared because most species were able to expand their ranges throughout the landscape (blue and green lines in d and e). As a result, the variation in geographic range size of these species also was reduced as most of them ended up with wide ranges (green and blue boxplots in f).

References:

Hassell, M. P. et al. 1976. Patterns of dynamical behaviour in single-species populations. — Journal of Animal Ecology 45: 471-486.

Henriques-Silva, R. et al. 2015. On the evolution of dispersal via heterogeneity in spatial connectivity. — Proceedings of the Royal Society B: Biological Sciences 282: 20142879.

Kubisch, A. et al. 2011. Density-dependent dispersal and the formation of range borders. — Ecography 34: 1002-1008.